

# Palaeolatitude and age of the Indo–Asia collision: palaeomagnetic constraints

Guillaume Dupont-Nivet,<sup>1,2</sup> Peter C. Lippert,<sup>3</sup> Douwe J.J. van Hinsbergen,<sup>4</sup> Maud J.M. Meijers<sup>1</sup> and Paul Kapp<sup>5</sup>

<sup>1</sup>Paleomagnetic Laboratory “Fort Hoofddijk”, Faculty of Geosciences, Utrecht University, Budapestlaan 17, 3584 CD Utrecht, The Netherlands.

E-mail: gdn@geo.uu.nl

<sup>2</sup>Key Laboratory of Orogenic Belts and Crustal Evolution, Ministry of Education, Peking University, Beijing 100871, China

<sup>3</sup>Department of Earth and Planetary Sciences, University of California, Santa Cruz, CA 95064, USA

<sup>4</sup>Physics of Geological Processes, University of Oslo, Sem Sælands vei 6, 0391 Oslo, Norway

<sup>5</sup>Department of Geosciences, University of Arizona, Tucson, Arizona 85721, USA

Accepted 2010 May 6. Received 2010 May 6; in original form 2010 March 15

## SUMMARY

Ongoing controversies on the timing and kinematics of the Indo–Asia collision can be solved by palaeomagnetically determined palaeolatitudes of terranes bounding the Indo–Asia suture zone. We show here, based on new palaeomagnetic data from the Linzizong volcanic rocks (54–47 Ma) near the city of Lhasa, that the latitude of the southern margin of Asia was  $22.8 \pm 4.2^\circ\text{N}$  when these rocks were deposited. This result, combined with revised palaeomagnetic results from the northernmost sedimentary units of Greater India and with apparent polar wander paths of India and Eurasia, palaeomagnetically constrain the collision to have occurred at  $46 \pm 8$  Ma (95 per cent confidence interval). These palaeomagnetic results are consistent with tomographic anomalies at  $15\text{--}25^\circ\text{N}$  that are interpreted to locate the Tethyan oceanic slab that detached following collision, and with independent 56–46 Ma collision age estimates inferred from the timing of slowing down of India, high pressure metamorphism, the end of marine sedimentation and the first occurrence of suture zone and arc detritus on the Greater Indian margin. When compared with apparent polar wander paths of India and Eurasia, the  $\sim 46$  Ma onset of collision at  $22.8 \pm 4.2^\circ\text{N}$  implies  $2900 \pm 600$  km subsequent latitudinal convergence between India and Asia divided into  $1100 \pm 500$  km within Asia and  $1800 \pm 700$  km within India.

**Key words:** Palaeomagnetism applied to tectonics; Continental tectonics: compressional; Asia.

## 1 INTRODUCTION

The Indo–Asia continental collision is one of the most profound tectonic events that occurred in Cenozoic time. According to climate and tectonic models, it resulted in the formation of the Himalayas and the Tibetan Plateau (Fig. 1a), the highest elevated landmass on Earth, which significantly altered regional environments and possibly global climate (Galy *et al.* 2007; Dupont-Nivet *et al.* 2008; Royden *et al.* 2008; Boos & Kuang 2010). These models rely on estimates of the timing and kinematics of the collision, which remain controversial despite decades of research (Aitchison *et al.* 2008; Garzanti 2008). The Indo–Asia collision occurred along the Indus–Yarlung suture zone separating the Lhasa terrane (the southernmost terrane of Asia, or ‘Greater Asia’) from the Tethyan Himalayas—generally interpreted to represent the northern margin of India, or ‘Greater India’. The collision is generally assumed to have been underway by 40–60 Ma based mainly on (1) the recognition of

Indian-affinity eclogitized sediments (55–48 Ma) in the northwestern Himalayas, (2) the end of marine sedimentation in the Tethyan Sequence of the northwestern Himalaya, (3) the first appearance of suture-zone and arc detritus in Tethyan and Himalayan foreland basin strata and (4) a dramatic slow-down of the India–Asia convergence rate (Leech *et al.* 2005; Zhu *et al.* 2005; Green *et al.* 2008; Guillot *et al.* 2008; Copley *et al.* 2010). However, this is challenged by propositions of a much younger ( $<35$  Ma) collision age based on reinterpretations of these observations and uncertainties in positioning Greater Asia and Greater India during the collision (Aitchison *et al.* 2007). In principle, the problem can be solved using palaeomagnetism to determine the latitudes through time of the colliding margins of Asia and India which are now incorporated in the orogenic belt (Achache *et al.* 1984; Besse *et al.* 1984; Klootwijk *et al.* 1992; Patzelt *et al.* 1996). Large uncertainties remain in existing palaeomagnetic data, and particularly those used to constrain the palaeolatitude of the southern margin of Asia (the Lhasa terrane,

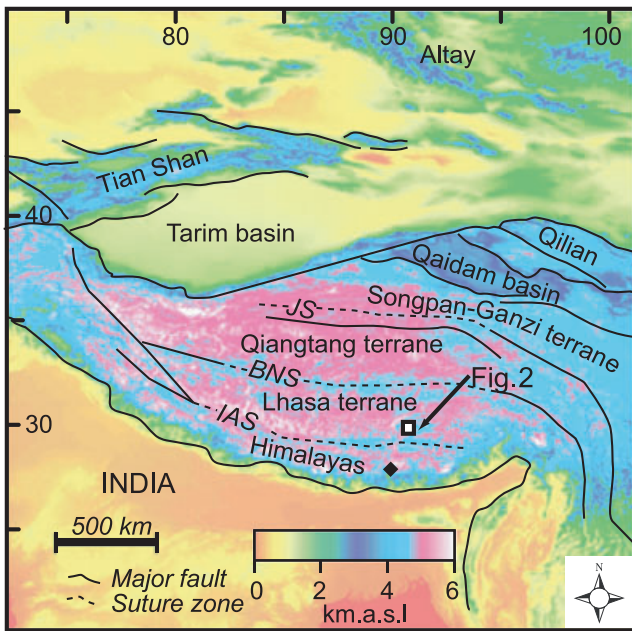


**Figure 1.** Location of sampling area of Fig. 2 (open white squares) on digital elevation model of the Indo-Asia collision zone (modified from Dupont-Nivet *et al.* 2008). Black diamond locates palaeomagnetic sites from Tethyan Himalayas (Patzelt *et al.* 1996). IAS, Indo-Asia suture; BNS, Bangong Nujiang suture; JS, Jinsha suture.

Fig. 1) before and during the collision. Existing palaeomagnetic data sets from volcanic and sedimentary rocks yield a wide range of palaeolatitude estimates from 5°N to 30°N (Westphal & Pozzi 1983; Achache *et al.* 1984; Lin & Watts 1988b; Chen *et al.* 1993; Liebke *et al.* 2010; Tan *et al.* 2010). This large disparity may be partly

attributed to low-latitude bias due to palaeomagnetic inclination shallowing during deposition and compaction of sediments (Tauxe 2005). Although volcanic rocks are in principle devoid of inclination shallowing, published volcanic data sets from the Lhasa terrane still provide conflicting results, primarily because these studies are based on too few data to confidently determine a palaeomagnetic pole at the time of collision (Achache *et al.* 1984; Lin & Watts 1988a; Tan *et al.* 2010). To better estimate the palaeolatitude of the southern margin of Asia and thus constrain the age of inception of the Indo-Asia collision as well as the magnitude of subsequent continental convergence, we provide in this paper new palaeomagnetic data from volcanic rocks of the Lhasa terrane.

## 2 PALAEOMAGNETIC RESULTS

### 2.1 Geological setting of sampled rocks

Sampled volcanic strata of the Linzizong Formation are part of the late Cretaceous to Palaeogene Gangdese arc found extensively on the southern Lhasa terrane (Lee *et al.* 2009). At Linzhou (Penbo), approximately 30 km north of Lhasa, ~2–3 km of the Linzizong Formation consists of four clastic to volcanic units and lie unconformably on the Cretaceous Takena formation and older strata. Palaeomagnetic sampling sites consist of seven to eight core samples oriented using magnetic and sun compasses. 32 palaeomagnetic sites (GL1–GL32) were collected from distinct and successive horizons of massive felsic welded tuff throughout a continuously exposed 1.5-km-thick section of the T2 unit (Fig. 2). Five additional sites (GS2, GS4, GS9, GS11 and GS22) were collected in silicic tuffaceous intervals at the top of the T2 unit where they are found interbedded with clastic red beds of the T3 unit. The stratigraphically lowest sampled horizon (GL32) in our section is dated  $53.9 \pm 1.4$  Ma and the highest (GS22) is less than 100 m above a flow unit dated

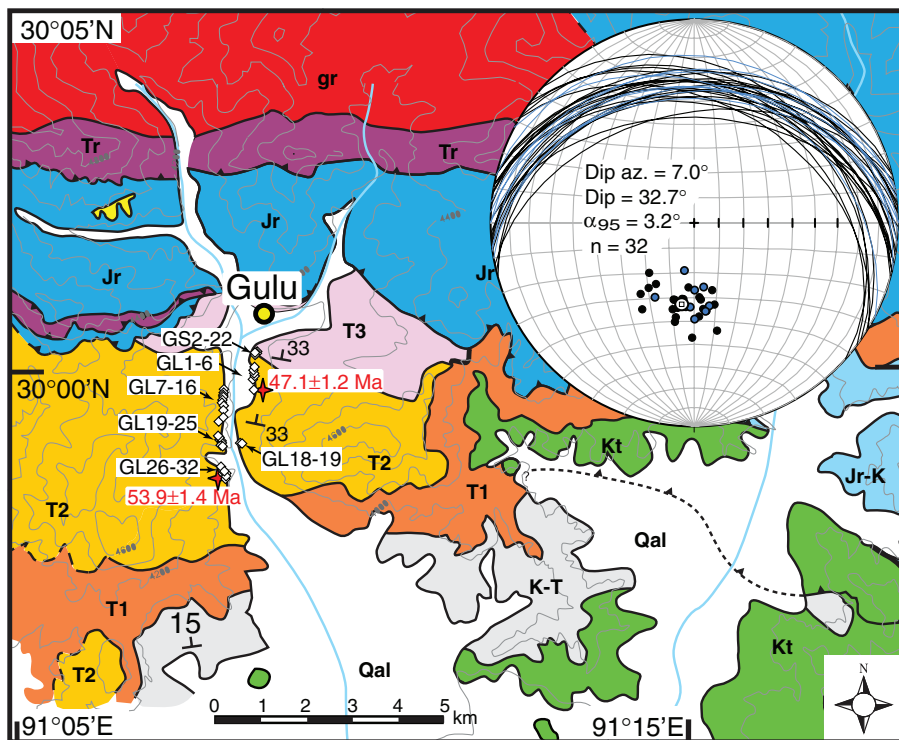


**Figure 2.** Palaeomagnetic sites location (white diamonds) on simplified geologic map near Linzhou (Penbo) with radiometric ages (red stars) of sampled T2 formation (detailed legend in He *et al.* (2007)).

at  $47.1 \pm 1.2$  Ma using U–Pb zircon dating (He *et al.* 2007). Bedding attitudes were measured at 23 locations throughout the section based on the planar orientations of the top surfaces of volcanic flows and interbedded sediments where available (Fig. 2; Table S1). Identical bedding attitudes were obtained by measuring both regional strike and dip clearly apparent in the non-vegetated landscape and by measuring the orientations of columnar joints (assumed to be perpendicular to palaeohorizontal) found at nine locations. The observed variations in the orientations of measured bedding are small and random throughout the sampled section. Therefore, a mean bedding correction (dip direction = N7.0°; dip = 32.7°;  $\alpha_{95}$  = 3.2°) was applied for the entire section in order to average out the uncertainty inherent to measuring the orientation of such volcanic deposits.

### 2.2 Palaeomagnetic analysis

Samples (standard 2.5 cm cylindrical specimens) were demagnetized using thermal and/or alternating field (AF) treatment at 17–25

successive steps from initial measurement of natural remanent magnetization (NRM) up to 680 °C or 90 milliTesla (mT) with an automated 2G RF-SQUID cryogenic magnetometer, in-line degausser and ASC Model TD48 oven in a shielded environment. Thermal and AF treatment yielded similar results (Fig. 3). After cleaning of a secondary overprint at low temperature/coercivity levels, most samples revealed a straightforward Characteristic Remanent Magnetization (ChRM) that is unblocked between 550 and 575 °C and 30–60 mT for thermal and AF treatment, respectively. Demagnetization behaviours and rock magnetic experiments suggest a simple magnetic mineralogy dominated by magnetite (Fig. 3). At some sites, however, there is evidence for an additional component with a lower unblocking temperature (<350 °C) but a higher coercivity (>60 mT). This may indicate the presence of Ti-rich titanomagnetite or alteration of the original magnetite (Dunlop & Özdemir 1997). Ti-rich titanomagnetite is a metastable mineral and thus its occurrence may indicate fresh and unaltered particles (Appel & Soffel 1984). Unfortunately, the component is insufficiently resolved in most samples to make sense of the directions it may

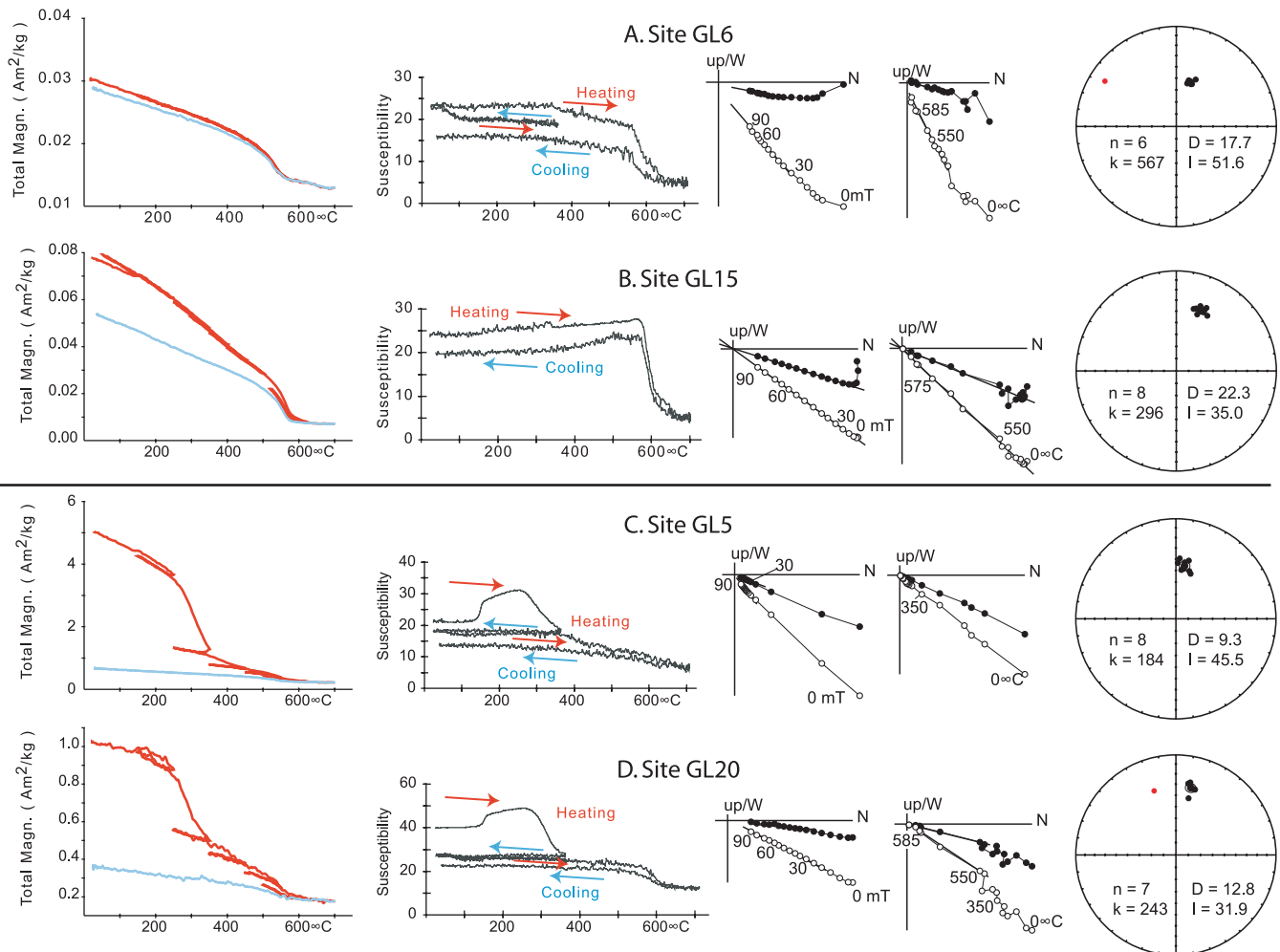


**Figure 3.** Rock magnetic data from typical samples of characteristic behaviours. Most samples (a and b) have typical magnetite behaviour but some samples show more complex behaviour (c and d) with a low temperature component possibly related to Ti-rich titanomagnetite and/or oxidation of primary magnetite. From left- to right-hand panels: high field thermomagnetic runs on Curie balance (Mullender *et al.* 1993); Low field thermomagnetic runs susceptibility vs. temperature on Kappabridge KLY3-CS; Demagnetization diagrams from AF in mTesla (left-hand panel) and thermal in degrees Celcius (right-hand panel), respectively, with full (open) circles are horizontal (vertical) projections (in stratigraphic coordinates); Stereographic projections of obtained ChRM directions from the considered site with black (open) symbols in lower (upper) hemisphere. Red are rejected outlying directions. Mean and 95 per cent confidence interval indicated. *n*, number of ChRM directions; *k*, precision parameter; *D*, mean declination; *I* = mean Inclination.

carry. Furthermore, because this component may also result from secondary magnetization, it was discarded from further ChRM analysis. The ChRM directional analysis was thus performed on the other component that was found in most samples.

Principal component analysis on at least five successive steps resulted in precisely determined ChRM directions for most samples. Five samples, however, had a ChRM direction with a Maximum Angular Deviation  $>5^\circ$ , and these were excluded from site mean direction calculations (Table S2). Another ten ChRM directions which are more than two angular standard deviation from the site-mean direction were also rejected. Site-mean directions with  $k < 50$  and  $n < 5$  were systematically discarded following volcanic data selection of (Johnson *et al.* 2008). A few site-mean directions from successive strata are statistically indistinguishable at the 95 per cent confidence level, suggesting that emplacement of these volcanic horizons outpaced palaeosecular variation (PSV). ChRM directions from these sites were combined into direction groups to avoid directional overrepresentation and ensure that each mean direction group represents an independent spot-reading of the palaeomagnetic field (Table S3).

Close inspection of the remaining 24 site-mean directions (Fig. 4) reveals that the four stratigraphically highest sites (GS2, GS11, GS22 and GS4 + 9) appear to have anomalously steep inclinations ( $10\text{--}30^\circ$  steeper than the overall locality mean). An unrecognized dip variation of this magnitude with respect to the other sites is unlikely because such a change in attitude would have been obvious in the continuously exposed stratigraphy that was carefully and consistently measured throughout the sampled interval (Fig. 2; Table S1). Also, syntilting magnetization may not explain this trend, because it would cause these stratigraphically highest sites to display shallower rather than steeper directions. Furthermore, the rock magnetic properties of the GS sites with steep inclinations are identical to the other nearby directly underlying sites (e.g. GL5 and GL6; Fig. 3), as expected since they are essentially the same type of rocks. Finally, because the virtual geomagnetic poles (VGP) of

these sites are within  $30^\circ$  from the mean, well within the range of secular variation (Johnson *et al.* 2008) we find no reason to exclude them based on the distribution of our data set (Fig. 4c).

We extend our data set by including previously obtained sites means from the Linzizong volcanic flows (Table S3): nine sites located exclusively in the upper part of the section near where we sampled the GS sites (Tan *et al.* 2010) and eight sites more regionally distributed with contrasting bedding attitudes (Achache *et al.* 1984). Out of the eight published site means of Achache *et al.* (1984), we rejected four site-means with  $n < 5$  and  $k < 50$  similarly to our site mean directions (Table S3). The nine exclusively normal sites mean directions of Tan *et al.* (2010) from the upper part of the section are tightly clustered with a VGP scatter ( $S = 10.3^\circ$ ) that is too low compared to the expected ( $S = 14.5^\circ$ ) value at  $20^\circ\text{N}$  (Johnson *et al.* 2008). It is clear that both these limited data sets do not, by themselves, provide a representative average of secular variation. However, they are statistically indistinguishable from our results and bracketed between a 65 and 45 Ma age span that includes our sampling interval. They therefore provide suitable complementary data that may be included in our data set. The resulting set of 37 independent site-means cluster in antipodal fashion with 30 normal and only 7 reversed polarity directions. virtual geomagnetic poles (VGP) calculated from the 37 independent site-means have a direction scatter ( $S = 14.3^\circ$ ) comparable to expected ( $S = 14.5^\circ$ ) values at  $20^\circ\text{N}$  (Johnson *et al.* 2008) indicating suitable representation of the palaeomagnetic field. The low representation of reversed directions clearly under-represent PSV and thus precludes rigorous application of the reversals test. However, site mean directions cluster after structural correction for a positive regional fold test (McFadden 1990) obtained at the 95 per cent confidence level, further suggesting the combined directions form a primary palaeomagnetic record.

The observed scatter in the large number of independent directions is consistent with the amount of dispersion expected for time-averaging secular variation (Johnson *et al.* 2008). Moreover,

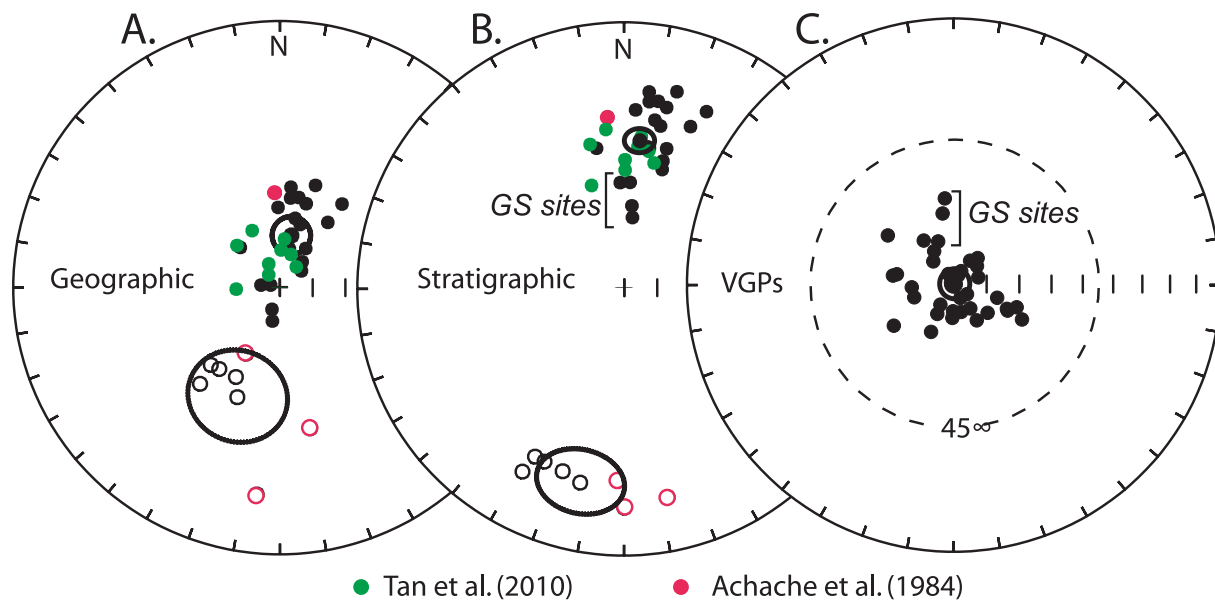


**Figure 4.** (a and b) Site-mean ChRM directions on equal area projections with full black (open white) symbols projected on the lower (upper) hemisphere before (Geographic) and after (Stratigraphic) tilt correction. Black ellipses are  $\alpha_{95}$  confidence on normal and reversed directions, respectively. Red – site means from Achache *et al.* (1984); green – site means from Tan *et al.* (2010). (c) Virtual Geomagnetic Poles (VGPs) of site mean directions (stratigraphic coordinates) centred on the mean of the VGPs (latitude =  $76.9^\circ\text{N}$ ; longitude =  $222.1^\circ\text{E}$ ;  $\alpha_{95} = 5.0^\circ$ ). The GS sites are well within  $45^\circ$  from the mean of the VGPs.

the large time span of the sampled section as determined from geochronologic studies and the recording of two magnetic reversals suggest our directions confidently provide a suitable representation of secular variation of the palaeomagnetic field at the time of rock emplacement. The mean of the combined 37 VGP directions can thus be used to calculate a reliable palaeolatitude for the southern Lhasa terrane at the time of Linzizong deposition.

### 3 IMPLICATIONS–DISCUSSION

#### 3.1 Palaeolatitude of the southern margin of Asia

Our result places the southern extent of the margin of Asia at  $22.8 \pm 4.2^\circ\text{N}$  between 54 and 47 Ma (for a reference point at the present-day position of the Indo–Asia suture at  $88^\circ\text{E}$ ,  $29^\circ\text{N}$ ; Fig. 2, Table 1). This palaeolatitude is in agreement with recent results from volcanic dykes intruding the Linzizong formation (Liebke *et al.* 2010), but significantly higher than previous estimates of the suture palaeolatitude ( $7 \pm 6^\circ\text{N}$ ) based mainly on upper Cretaceous sediments (Chen *et al.* 1993). We attribute this discrepancy to shallowing of palaeomagnetic inclination in the upper Cretaceous sediments that is typically observed in Asian red beds (Dupont-Nivet *et al.* 2002; Tauxe 2005). This interpretation is supported by recent results from sediments and volcanics from the upper Cretaceous Takena formation (Tan *et al.* 2010) which show inclinations  $>15^\circ$  steeper in presumed coeval volcanics than in the Takena sediments. The sedimentary and volcanic-based inclinations are consistent after the elongation/inclination (E/I) correction method (see below) is applied to the sedimentary data sets (Tauxe 2005), further suggesting sedimentary inclination shallowing by flattening is significant.

We combine available results from upper Cretaceous volcanic flows of the Lhasa terrane (Lin & Watts 1988b; Tan *et al.* 2010) to calculate a Cretaceous latitude of the southern margin of Asia of  $20.5 \pm 6.0^\circ\text{N}$  (see Table S4 and Fig. 4). The palaeolatitude for the southern margin of Eurasia calculated from the apparent polar wander path is  $32.2 \pm 2.6^\circ\text{N}$  (Torsvik *et al.* 2008), indicating that the latitudinal distance of the suture with respect to Eurasia ( $\Delta D$ ) during the upper Cretaceous was  $1100 \pm 700$  km. This result is remarkably consistent both with the shallowing-corrected upper Cretaceous Takena sediments ( $\Delta D = 1100 \pm 400$  km) and our lower Palaeogene results from the Linzizong formation ( $\Delta D = 1100 \pm 500$  km; see Tables 1 and S4). This excellent result, however, does imply that most of the intra-Asian convergence occurred after the collision and that precollisional intra-Asian shortening is limited to within palaeomagnetic uncertainties. In addition, the calculated  $\sim 20^\circ\text{N}$  palaeolatitudes for the suture zone since the Cretaceous are consistent with the  $15\text{--}25^\circ\text{N}$  latitude range of high velocity seismic tomography anomalies in the mantle below India previously interpreted as remnants of subducted Neo-Tethyan lithosphere that detached upon collision (Van der Voo *et al.* 1999; Fig. 3).

#### 3.2 Timing of Indo–Asia collision

To estimate the age of the onset of collision, we assess the timing at which the palaeolatitude of the southern margin of Asia defined by our results, overlaps with the palaeomagnetically determined palaeolatitude estimates from the Tethyan Himalayan sediments taken to represent the northern extent of Greater India (note this is a minimum age estimate since Tethyan Himalayan sediments could have been deposited some distance south of the northern margin of Greater India).

**Table 1.** Palaeomagnetic data sets constraining the palaeolatitude of the Lhasa terrane and the Tethyan Himalaya.

Data set	Location			Observed pole				Reference pole				Palaeolatitude				Latitudinal Convergence								
	Lat (°N)	Long (°E)	Age (Ma)	Lat (°N)	Long (°E)	Age (Ma)	n	Age (Ma)	Lat (°N)	Long (°E)	Age (Ma)	Lat (°N)	Long (°E)	Age (Ma)	Plat <sub>o</sub> (°N)	Plat <sub>e</sub> (°N)	Suture (°N)	Plat <sub>s</sub> (°N)	ΔPlat (°N)	ΔD (km)	References			
																						Ave. (Ma)	Min. (Ma)	Max (Ma)
Lhasa terrane																								
Linzizong volc.	30.0	91.1	50.5	47.0	54.0	81.2	221.4	4.2	37	50	79.1	154.2	2.6	24.1	± 4.2	34.4	± 2.6	22.8	± 4.2	-10.3	± 4.9	-1100	± 500	1,2,3
Takena fm. <sup>a</sup>	30.0	91.1	87.5	65.0	110.0	76.7	327.1	2.5	377	90	80.3	169.1	2.6	22.0	± 2.5	31.5	± 2.6	21.6	± 2.5	-9.5	± 3.6	-1100	± 400	3
K volcanics	30.7	91.2	95.0	85.0	105.0	76.3	213.8	6.0	29	90	80.3	169.1	2.6	22.7	± 6.0	32.2	± 2.6	20.5	± 6.0	-9.5	± 6.5	-1100	± 700	3,4
Tethyan Himalaya																								
Zongpu <sup>a</sup>	28.3	88.5	59.0	55.0	63.0	68.2	277.1	3.1	101	60	51.6	276.4	5.7	6.7	± 3.1	-9.8	± 5.7	7.4	± 3.1	16.5	± 6.5	1800	± 700	5
Zongshan <sup>a</sup>	28.3	88.5	68.0	65.0	71.0	55.8	261.6	3.5	144	70	39.0	279.6	5.0	-5.7	± 3.5	-21.9	± 5.0	-5.0	± 3.5	16.2	± 6.1	1800	± 700	6
Collision			45.7	37.9	53.9													22.8	± 4.2					

*Notes:* Data set – palaeomagnetic data set from a locality; Location – latitude (Lat) and longitude (Long) of the locality; Observed Pole – age range of sampled rocks; latitude (Lat), longitude (Long) and radius of 95 per cent confidence circle ( $A_{95}$ ) of mean observed Virtual Geomagnetic Pole (VGP) for the locality; Reference Pole – age, latitude (Lat), longitude (Long) and radius of 95 per cent confidence circle ( $A_{95}$ ) from palaeomagnetic Apparent Polar Wander Path for Eurasia or India as indicated (Torsvik *et al.* 2008); Palaeolatitude – locality palaeolatitude (Plat) derived from observed pole; Expected palaeolatitude (Plat<sub>e</sub>) derived from reference pole; Suture palaeolatitude (Plat<sub>s</sub>) derived from observed pole at the reference point set at present-day position of the Indo–Asia suture ( $88^\circ\text{E}$ ,  $29^\circ\text{N}$ ) – latitudinal convergence – observed minus expected palaeolatitude ( $\Delta\text{Plat}$ ) converted into distance ( $\Delta D$ ) rounded to nearest hundred kilometres; error from Gaussian propagation ( $\sum A_{95}^2$ )<sup>1/2</sup>. Ref. – reference of data set: 1 – this study; 2 – Achache *et al.* (1984); 3 – Tan *et al.* (2010); 4 – Lin & Watts (1988a,b); 5 – Patzelt *et al.* (1996); Collision – collision age derived from the intersection of the latitude of Lhasa terrane with the APWP of India (Torsvik *et al.* 2008) shifted north by constant average  $\Delta\text{Plat} = 16.35^\circ$ , with the latitude of Lhasa terrane.  
<sup>a</sup>Sediments corrected for inclination shallowing.

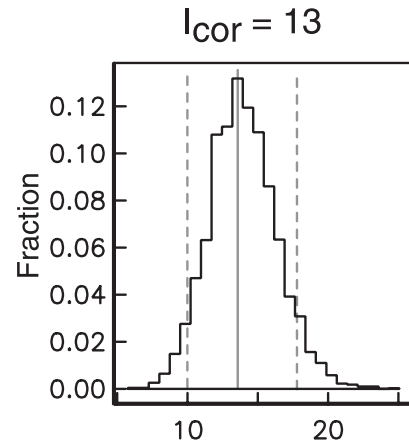
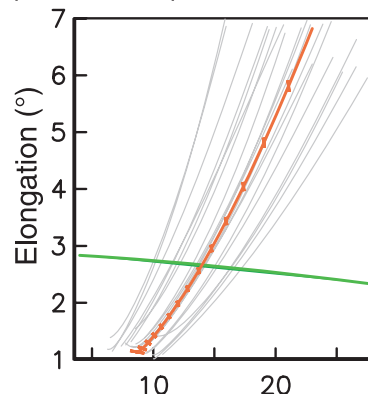
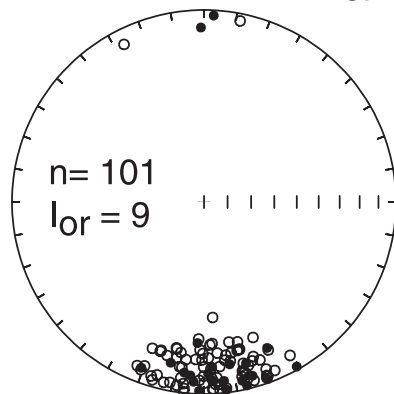
The palaeolatitude of the northern Greater Indian margin is calculated from palaeomagnetic data collected directly south of the Indo–Asia suture (Fig. 1a) from sites at Zongpu (63–55 Ma) and at Zongshan (71–65 Ma). These palaeomagnetic results come from shallow-marine limestones in the uppermost part of the Tethyan Himalayan sequence (Patzelt *et al.* 1996) and supersede previous studies of those rocks (Besse *et al.* 1984; Klootwijk 1984). Patzelt *et al.* (1996) assumed that their palaeomagnetic data are not affected by inclination shallowing because the limestone lithology is less prone to compaction. However, Patzelt *et al.* (1996) had no numerical procedures available at the time of their study to verify that assumption. Here we evaluate the possibility of inclination shallowing affecting these data sets by applying the E/I correction method (Tauxe 2005).

The E/I method is based on statistical models of geomagnetic palaeosecular variation and is only applicable to data sets with large numbers ( $n \geq 100$ ) of independent measurements of the geomagnetic field. The corrected data set is obtained by incrementally ‘unflattening’ the observed directions following the flattening factor formula of King (1955) and by determining when both the average inclination and elongation of the distribution of directions are most consistent with the expected values from the reference statistical ge-

omagnetic model (for detailed method description, see Tauxe 2005; Tauxe & Kent 2004). If the E/I method reveals significant elongation in the distribution of magnetic field directions consistent with sedimentary inclination shallowing, then the steeper E/I corrected inclination may provide (within confidence limits) a more realistic estimate of the original inclination.

We apply the E/I correction method to the original data sets of Patzelt *et al.* (1996) which have 101 and 144 ChRM directions from the Zongpu and Zongshan localities, respectively. These directions are from individual samples each collected from different sedimentary horizons and therefore satisfy the requirement that each direction is an independent sample of the geomagnetic field. The recursive cut-off method (Vandamme 1994) was applied on separate sets of reverse and normal polarity populations from each formation prior to performing the E/I correction to evaluate for the presence of any outlier or transitional magnetic directions. A few widely outlying directions were discarded from further analysis. For both data sets, application of the E/I correction yielded only small inclination corrections ( $<5^\circ$ ) resulting in palaeolatitude positions essentially similar to the original results before correction (Fig. 5). The near absence of correction as determined from the E/I method suggests that these Tethyan Himalayan sediments have not been

### A. Greater India: Zongpu (55–63 Ma)



### B. Greater India: Zongshan (65–71 Ma)

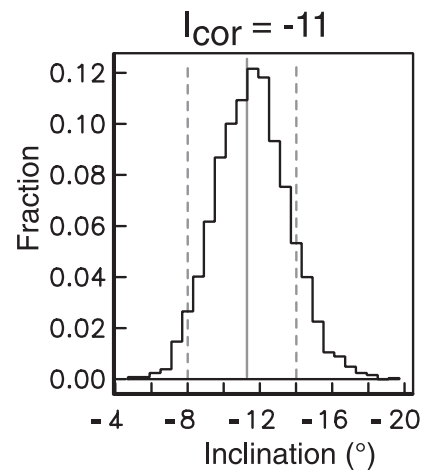
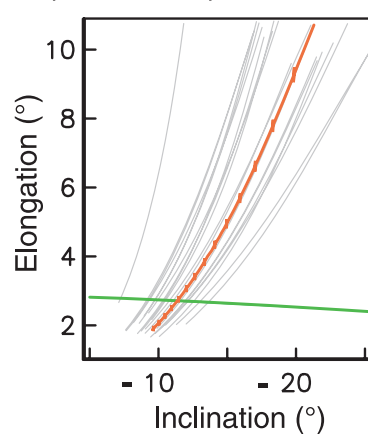
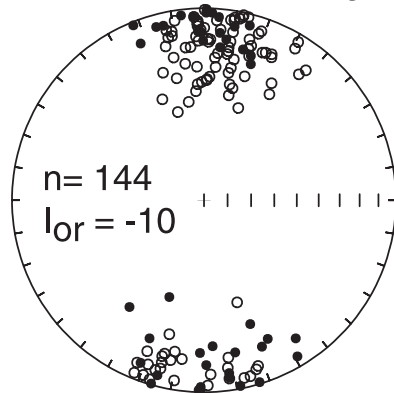


**Figure 5.** Sedimentary data sets from the Tethyan Himalaya (Patzelt *et al.* 1996) corrected for inclination shallowing using the Elongation/Inclination method (Tauxe 2005). Left-hand panel: stereographic projection in stratigraphic coordinates of  $n$  individual ChRM directions.  $I_{or}$  is original mean inclination before correction. Centre panel: thick red line is the range of elongation–inclination obtained upon applying a range of flattening factors (King 1955) on the original data set. Thin green line is expected inclination–elongation pairs according to Tauxe (2005). The intersection defines the corrected inclination. Right-hand panel: probability histogram of corrected inclination ( $I_{cor}$ ) from bootstrap analysis. Dashed lines indicate 95 per cent confidence interval.

affected by significant inclination shallowing, thus supporting the original assumption of Patzelt *et al.* (1996).

The youngest of these data sets indicates that the Tethyan Himalayan sediments were located  $7.4 \pm 3.1^\circ\text{N}$  at  $59 \pm 4$  Ma, clearly much farther south than the southern margin of Asia (Figs 6 and 7, Table 1). Thus, the collision between the Tethyan Himalayas and the Lhasa Block could not have occurred before  $59 \pm 4$  Ma. We note the remarkable constancy through time of the latitudinal distance between the Tethyan Himalayan sediments and the northward path of the Indian continent ( $\Delta D = 1800 \pm 700$  km at 65–71 Ma vs.  $1800 \pm 700$  km at 55–63 Ma). This observation suggests that

Greater India moved coherently with the Indian continent before collision. To estimate the age of the collision, we thus extrapolate the northward path of India through the palaeolatitudes of the Tethyan Himalayas until they intersect with the palaeolatitudes of the southern Lhasa margin at  $22.8 \pm 4.2^\circ\text{N}$  (Fig. 2). This provides a 46 Ma minimum age for the collision with 95 per cent confidence interval between 38 Ma and 54 Ma (Table S3). The palaeomagnetic constraints thus precludes the possibility that collision began after 35 Ma at the longitude of Lhasa (Aitchison *et al.* 2008), but is in excellent agreement with independent, albeit indirect evidence suggesting collision began between 56 and 46 Ma (Fig. 6): (1) the

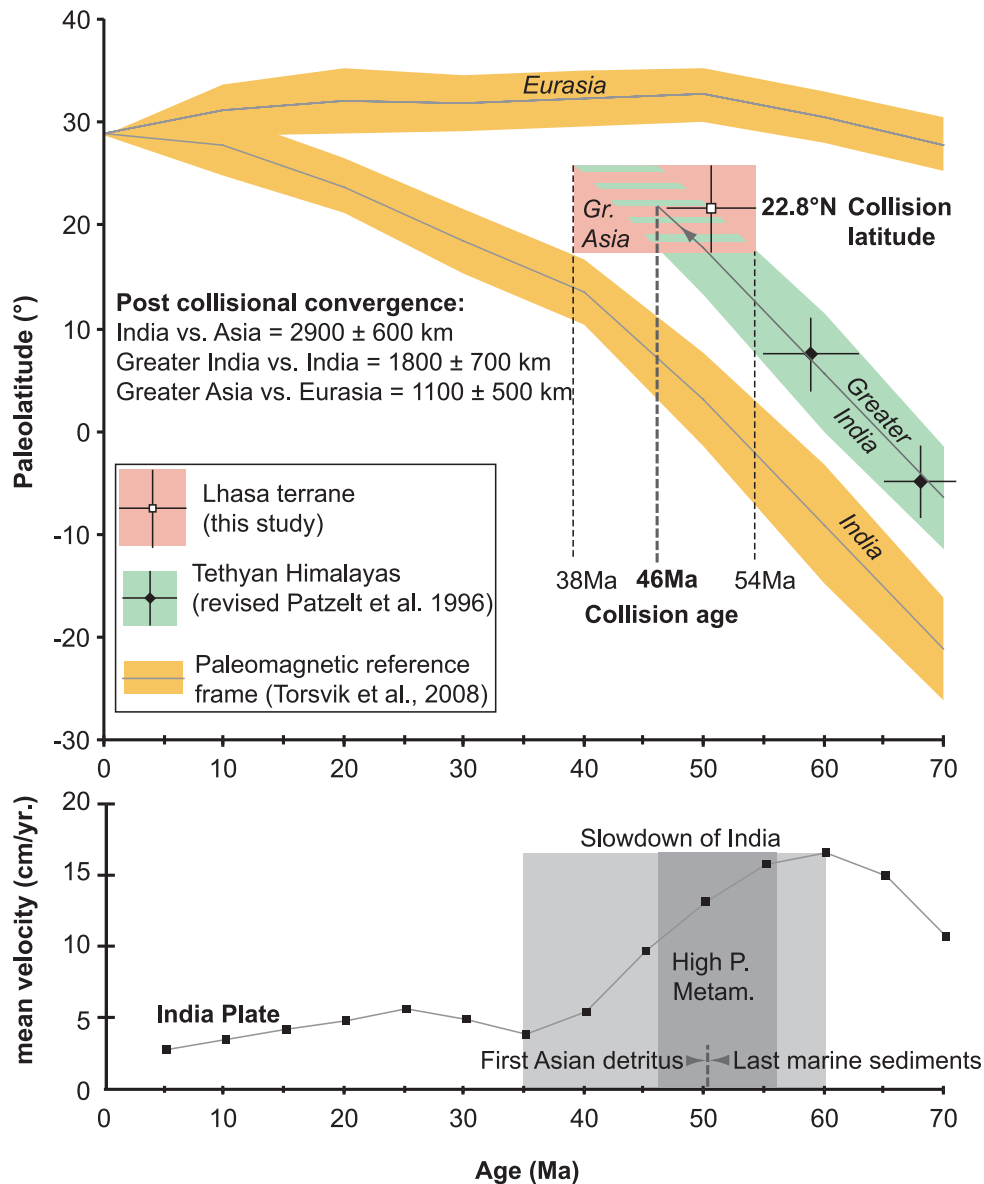


**Figure 6.** Upper diagram: Palaeolatitudes of the southern margin of Asia (open square, this study) and the northern margin of greater India (black diamond, original data of Patzelt *et al.* (1996) corrected with E/I method of Tauxe (2005)) provided by palaeomagnetic results from rocks of the Lhasa terrane and the Tethyan Himalayas, respectively (Table 1). Error bounds display 95 per cent confidence interval on latitude and age range of analysed rocks. The India and Eurasia latitudinal paths with 95 per cent confidence interval (shaded yellow areas) of calculated from the synthetic Apparent Polar Wander Path of Torsvik *et al.* (2008). The age of the collision is estimated using the intersection between the palaeolatitude of the southern margin of the Lhasa terrane with the path of India fitted through the palaeolatitudes of the Tethyan Himalayas (green shaded area, Table 1). Lower diagram: absolute velocity of India according to the palaeomagnetic global apparent polar wander path of Torsvik *et al.* (2008). Other evidence for suturing is indicated: high pressure metamorphism at 46–56 Ma (Guillot *et al.* 2008), last occurrence of marine sediments at 50.5 Ma (Green *et al.* 2008) and first occurrence of presumed Asian detritus on the Indian plate at  $50.6 \pm 0.2$  Ma (Zhu *et al.* 2005).

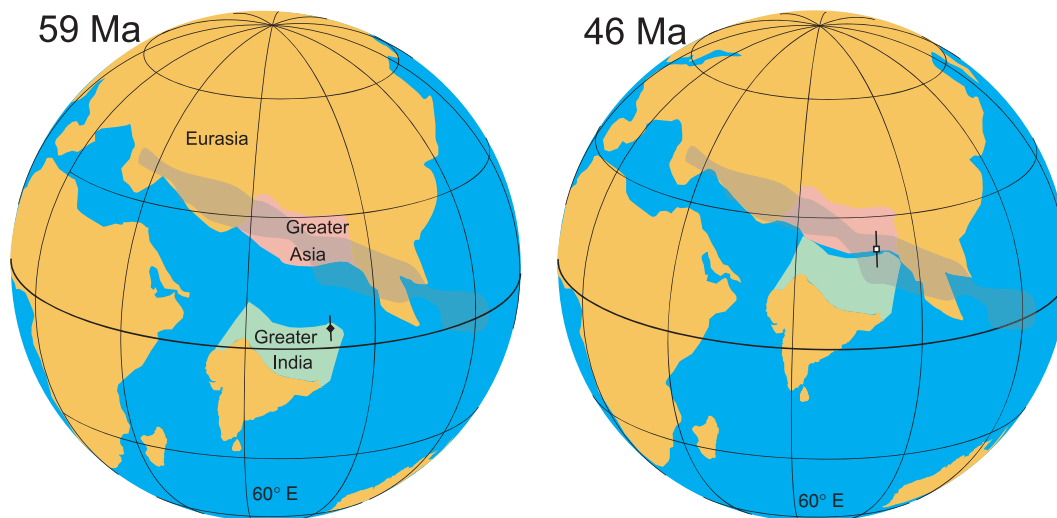


**Figure 7.** Palaeo-reconstructions based on palaeomagnetic constraints showing the extent of the southern margin of Asia (Greater Asia) at the onset of the Indo–Asia collision ca. 46 Ma (this study) and the extent of Greater India at 59 Ma (Patzelt *et al.* 1996) with respect to reference positions of India and Eurasia (Torsvik *et al.* 2008). Shaded area locates the high velocity tomography anomaly previously interpreted as slab remnants subducted during Neo-Tethys closure between India and Tibet (i.e. mantle anomaly II of (Van der Voo *et al.* 1999).

slowing down of India relative to Asia at  $\sim 50$  Ma (Copley *et al.* 2010), (2) high pressure metamorphism of Indian-affinity continental rocks in the northwestern Himalaya at 46–56 Ma (Guillot *et al.* 2008, 2007), (3) the last occurrence of marine sediments at 50.5 Ma in the NW Himalaya (Green *et al.* 2008) and (4) the first occurrence of ophiolitic detritus in Tethyan Himalayan sediments at  $50.6 \pm 0.2$  Ma (Zhu *et al.* 2005).

### 3.3 Post-collisional convergence

The onset of collision at  $\sim 46$  Ma implies a subsequent latitudinal convergence of  $2900 \pm 600$  km ( $27.7 \pm 5.2^\circ$ ) between India and Eurasia according to the apparent polar wander path (APWP) describing these plate motions (Torsvik *et al.* 2008). The collision palaeolatitude at  $22.8 \pm 4.2^\circ$ N further implies the total latitudinal convergence was accommodated by  $1100 \pm 500$  km ( $10.3 \pm 4.9^\circ$ ) between southern Tibet and stable Eurasia and  $1800 \pm 700$  km ( $16.2 \pm 6.5^\circ$ ) between the Tethyan Himalaya and stable India (Fig. 6, Table 1).

The intra-Eurasia latitudinal convergence of  $1100 \pm 500$  km is significantly lower than what previous palaeolatitude estimates of the southern margin of Asia imply. For example, using the previously proposed  $7 \pm 6^\circ$ N palaeolatitude (Chen *et al.* 1993) predicts  $2900 \pm 700$  km with respect to the APWP of Eurasia (Torsvik *et al.* 2008). Our result of  $1100 \pm 500$  km is, within error, comparable to the  $\sim 700$  km N–S crustal shortening that can be accounted for by structures north of the Indus–Yarlung suture (Avouac *et al.* 1993; Yin and Harrison, 2000; Guillot *et al.* 2003; Kapp *et al.* 2005b; Spurlin *et al.* 2005; Yin *et al.* 2008). The seemingly higher  $1100 \pm 500$  km convergence may be further reconciled with the  $\sim 700$  km N–S crustal shortening by recent palaeomagnetic studies on Cenozoic volcanics from stable Asia, which indicate that Asian palaeolatitudes from 50 to 20 Ma may be  $\sim 5$ – $10^\circ$  lower than predicted by Eurasian reference poles. Proposed mechanisms potentially responsible for these low latitudes such as non-dipolar field contribution or southerly position of Asia with respect to the Eurasian APWP are still debated (Chauvin *et al.* 1996; Hankard *et al.* 2007; Dupont-Nivet *et al.* 2010).

Within Greater India, the post-collisional latitudinal convergence of  $1800 \pm 700$  km greatly exceeds minimum shortening estimates of Indian-affinity rocks in the Himalayan thrust belt that are only on the order of  $\sim 700$  km (Yin & Harrison 2000; DeCelles *et al.* 2002; Long *et al.* in press). This requires that a large part of the Greater Indian lithosphere and crust by-passed the subduction zone without accretion. In other words, large volumes of Greater Indian lithosphere must have been subducted without leaving any remnants at the surface. In analogy to the Aegean orogen in the Mediterranean where 2400 km of convergence between alternating narrow continental and oceanic intervals within a single slab did not lead to multiple sutures (van Hinsbergen *et al.* 2005), we propose that a large part of Greater India consisted of thinned continental or even oceanic lithosphere. This may explain the enigmatic persistence of arc-type magmatism within the Gangdese arc until  $\sim 40$  Ma (Kapp *et al.* 2005a; Lee *et al.* 2009).

## 4 CONCLUSIONS

Recent advances in rock magnetism and geomagnetism show that palaeomagnetic records can provide reliable and consistent palaeolatitudes if (1) sedimentary data sets are corrected for inclination shallowing (Tauxe 2005) and (2) volcanic data sets are composed of sufficient independent high-quality readings of the palaeomagnetic field to average secular variations (Johnson *et al.* 2008). From the well-dated 54–47 Ma Linzizong volcanic successions directly north of the India–Asia suture zone, we provide independent palaeomagnetic site-mean directions passing high quality criteria ( $k > 50$  and  $n \geq 5$ ) in sufficient amount (37 sites) and with appropriate dispersion ( $S = 14.3$ ) to demonstrably characterize the expected time-averaged behaviour of the geomagnetic field. This large data set includes and supersedes previous palaeomagnetic Linzizong volcanic studies based on insufficient data sets with only four (Achache *et al.* 1984) and nine (Tan *et al.* 2010) reliable site-mean directions yielding, respectively: too low or too high palaeolatitudes, too high or too low post collisional convergence, and too old or too young collision ages. Here, with the combined 37 site-mean directions from lavas that are in principle immune to inclination shallowing biases,



we can reliably derive a palaeolatitude of  $22.8 \pm 4.2^\circ\text{N}$  for the southern margin of Asia at the time of Linzizong deposition (54–47 Ma). This implies  $1100 \pm 500$  km of latitudinal convergence within Asia since the collision, which is remarkably consistent with palaeolatitudes derived from revised data sets (Table 1, Table S4) from upper Cretaceous volcanics and shallowing-corrected inclination from sediments of the Lhasa terrane (Tan *et al.* 2010). Furthermore, when compared to shallowing-corrected inclination from sediments of the Tethyan Himalayas taken to represent the northern extent of Greater India, this Lhasa terrane palaeolatitude implies that collision between Greater India and Asia began at  $46 \pm 8$  Ma.

## ACKNOWLEDGMENTS

This research was funded by the Netherland Organization for Scientific Research (NWO) and ISES. D.J.J.v.H. acknowledges financial support from Statoil (SPLates Project). Erwin Appel, Eduardo Garzanti, Ursina Liebke and two other anonymous reviewers greatly improved the original manuscript. We thank Norbu Richen for field assistance, Kees Lenferink for lab assistance, Trond Torsvik for plate reconstruction material, Erwin Appel for sharing Tethyan Himalaya data sets, and Cor Langereis and Mark Dekkers for discussions.

## REFERENCES

- Achache, J., Courtillot, V. & Zhou, Y.X., 1984. Paleogeographic and tectonic evolution of southern Tibet since middle Cretaceous time: new paleomagnetic data and synthesis, *J. geophys. Res.*, **89**, 10 311–10 339.
- Aitchison, J.C., Ali, J.R. & Davis, A.M., 2007. When and where did India and Asia collide?, *J. geophys. Res.*, **112**, B05423, doi:10.1029/2006JB004706.
- Aitchison, J.C., Ali, J.R. & Davis, A.M., 2008. Reply to comment by Eduardo Garzanti on “When and where did India and Asia collide?”, *J. geophys. Res.*, **113**, B04412, doi:10.1029/2007JB005431.
- Appel, E. & Soffel, H.C., 1984. Model for the domain state of Ti-rich titanomagnetites, *Geophys. Res. Lett.*, **11**, 189–192.
- Avouac, J.P., Tapponnier, P., Bai, M., You, H. & Wang, G., 1993. Active thrusting and folding along the northern Tien Shan and Late Cenozoic rotation of the Tarim relative to Dzungaria and Kazakhstan, *J. geophys. Res.*, **98**, 6755–6804.
- Besse, J., Courtillot, V., Pozzi, J.P., Westphal, M. & Zhou, Y.X., 1984. Paleomagnetic estimates of crustal shortening in the Himalayan thrusts and Zangbo suture, *Nature*, **311**, 621–626.
- Boos, W.R. & Kuang, Z., 2010. Dominant control of the South Asian monsoon by orographic insulation versus plateau heating, *Nature*, **463**, 218–222, doi:10.1038/nature08707.
- Chauvin, A., Perroud, H. & Bazhenov, M.L., 1996. Anomalous low palaeomagnetic inclinations from Oligocene–Lower Miocene red beds of the south-west Tien Shan, Central Asia, *Geophys. J. Int.*, **126**, 303–313.
- Chen, Y., Cogne, J.-P., Courtillot, V., Tapponnier, P. & Zhou, X.Y., 1993. Cretaceous paleomagnetic results from western Tibet and tectonic implications, *J. geophys. Res.*, **98**, 17 981–18 000.
- Copley, A., Avouac, J.P. & Royer, J.Y., 2010. The India–Asia collision and the Cenozoic slowdown of the Indian plate: implications for the forces driving plate motions, *J. geophys. Res.*, **115**, doi:10.1029/2009JB006634.
- DeCelles, P.G., Robinson, D.M. & Zandt, G., 2002. Implications of shortening in the Himalayan fold-thrust belt for uplift of the Tibetan Plateau, *Tectonics*, **21**, 1062, doi:10.1029/2001TC001322.
- Dunlop, D. & Özdemir, Ö. 1997. *Rock Magnetism: Fundamentals and Frontiers*, pp. 573, Cambridge University Press, Cambridge.
- Dupont-Nivet, G., Guo, Z., Butler, R.F. & Jia, C., 2002. Discordant paleomagnetic direction in Miocene rocks from the central Tarim Basin: evidence for local deformation and inclination shallowing, *Earth planet. Sci. Lett.*, **199**, 473–482.
- Dupont-Nivet, G., Hoorn, C. & Konert, M., 2008. Tibetan uplift prior to the Eocene–Oligocene climate transition: evidence from pollen analysis of the Xining Basin, *Geology*, **36**, 987–990, doi:10.1130/GS25063A.1.
- Dupont-Nivet, G., Van Hinsbergen, D.J.J. & Torsvik, T.H., 2010. Persistently low Asian paleolatitudes: implications for the Indo–Asia collision, *Tectonics*, doi:10.1029/2008TC002437, in press.
- Galy, V., France-Lanord, C., Beyssac, O., Faure, P., Kudrass, H. & Palhol, F., 2007. Efficient organic carbon burial in the Bengal fan sustained by the Himalayan erosional system, *Nature*, **450**, 407–410, doi:10.1038/nature06273.
- Garzanti, E., 2008. Comment on “When and where did India and Asia collide?” by Jonathan C. Aitchison, Jason R. Ali & Aileen M. Davis, *J. geophys. Res.*, **113**, B04411, doi:10.1029/2007JB005276.
- Green, O.R., Searle, M.P., Corfield, R.I. & Corfield, R.M., 2008. Cretaceous–tertiary carbonate platform evolution and the age of the India–Asia collision along the Ladakh Himalaya (Northwest India), *J. Geol.*, **116**, 331–353, doi:10.1086/588831.
- Guillot, S., Garzanti, E., Baratoux, D., Marquer, D., Mahéo, G. & de Sigoyer, J., 2003. Reconstructing the total shortening history of the NW Himalaya, *Geochem. Geophys. Geosyst.*, **4**, 1064.
- Guillot, S., Replumaz, A., Hattori, K.H. & Strzeczynski, P., 2007. Initial geometry of western Himalaya and ultrahigh-pressure metamorphic evolution, *J. Asian Earth Sci.*, **30**, 557–564.
- Guillot, S., Mahéo, G., de Sigoyer, J., Hattori, K.H. & Pêcher, A., 2008. Tethyan and Indian subduction viewed from the Himalayan high-to ultrahigh-pressure metamorphic rocks: tectonophysics, Asia out of Tethys, *Geochron., Tectonic Sediment. Records*, **451**, 225–241.
- Hankard, F., Cogné, J.P., Kravchinsky, V.A., Carpozen, L., Bayasgalan, A. & Lkhagvadorj, P., 2007. New Tertiary paleomagnetic poles from Mongolia and Siberia at 40, 30, 20, and 13 Ma: Clues on the inclination shallowing problem in central Asia, *J. geophys. Res.*, **112**, B02101, doi:10.1029/2006JB004488.
- He, S., Kapp, P., DeCelles, P.G., Gehrels, G.E. & Heizler, M., 2007. Cretaceous–Tertiary geology of the Gangdese Arc in the Linzhou area, southern Tibet, *Tectonophysics*, **433**, 15–37.
- Johnson, C.L., *et al.* 2008. Recent investigations of the 0–5 Ma geomagnetic field recorded by lava flows, *Geochem. Geophys. Geosyst.*, **9**, doi:10.1029/2007GC001696.
- Kapp, J.L.D., Harrison, T.M., Kapp, P., Grove, M., Lovera, O.M. & Ding, L., 2005a. The Nyainqentanglha Shan: a window into the tectonic, thermal, and geochemical evolution of the Lhasa block, southern Tibet, *J. geophys. Res.*, **110**, B08413, doi:10.1029/2004JB003330.
- Kapp, P., Yin, A., Harrison, T.M. & Ding, L., 2005b. Cretaceous–Tertiary shortening, basin development, and volcanism in central Tibet, *Geol. Soc. Am. Bull.*, **117**, 865–878.
- King, R.F., 1955. The remanent magnetism of artificially deposited sediments, *Mon. Not. R. astr. Soc.*, Geophys. Supp., 115–134.
- Klootwijk, C.T., 1984. A review of Indian Phanerozoic paleomagnetism: implications for the Indo–Asia collision, *Tectonophysics*, **105**, 331–353.
- Klootwijk, C.T., Gee, J.S., Peirce, J.W., Smith, G.M. & McFadden, P.L., 1992. An early India–Asia contact: paleomagnetic constraints from Ninetyeast Ridge, OPD Leg 121, *Geology*, **20**, 395–398.
- Lee, H.-Y., Chung, S.-L., Lo, C.-H., Ji, J., Lee, T.-Y., Qian, Q. & Zhang, Q., 2009. Eocene Neotethyan slab breakoff in southern Tibet inferred from the Linzizong volcanic record: tectonophysics; continental collision, partial melting and ductile deformation in The Tibetan–Himalayan Orogenic Belt, *Tectonophysics*, **477**, 20–35.
- Leech, M.L., Singh, S., Jain, A.K., Klemperer, S.L. & Manickavasagam, R.M., 2005. The onset of India–Asia continental collision: early, steep subduction required by the timing of UHP metamorphism in the western Himalaya, *Earth planet. Sci. Lett.*, **234**, 83–97.
- Liebke, U., Appel, E., Neumann, U., Antolin, B., Lin, D. & Qiang, X., 2010. Position of the Lhasa terrane prior to India–Asia collision derived from palaeomagnetic inclinations of 53 Ma old dykes of the Linzhou Basin: constraints on the age of collision and post-collisional shortening within the Tibetan Plateau, *Geophys. J. Int.*, doi:10.1111/j.1365-246X.2010.04698.x, in press (this issue).

- Lin, J. & Watts, D.R., 1988a. Paleomagnetic constrains on Himalayan-Tibetan tectonic evolution, *Phil. Trans. R. Soc. Lond.*, **326**, 177–188.
- Lin, J. & Watts, D.R., 1988b. Paleomagnetic results from the Tibetan plateau, *R. Soc. Lond. Phil. Trans.*, **327**, 239–262.
- McFadden, P.L., 1990. A new fold test for palaeomagnetic studies, *Geophys. J. Int.*, **103**, 163–169.
- Mullender, T.A.T., van Velzen, A.J. & Dekkers, M., 1993. Continuous drift correction and separate identification of ferromagnetic and paramagnetic contribution in thermomagnetic runs, *Geophys. J. Int.*, **114**, 663–672.
- Patzelt, A., Li, H., Wang, J. & Appel, E., 1996. Palaeomagnetism of Cretaceous to Tertiary sediments from southern Tibet: evidence for the extent of the northern margin of India prior to the collision with Eurasia, *Tectonophysics*, **259**, 259–284.
- Royden, L.H., Burchfiel, B.C. & Van Der Hilst, R.D., 2008. The geological evolution of the Tibetan Plateau, *Science*, **321**, 1054–1058, doi:10.1126/science.1155371.
- Spurlin, M.S., Yin, A., Horton, B.K., Zhou, J. & Wang, J., 2005. Structural evolution of the Yushu-Nangqian region and its relationship to syncol-lisional igneous activity, east-central Tibet, *Geol. Soc. Am. Bull.*, **117**, 1293–1317; doi:10.1130/B25572.1.
- Tan, X., Gilder, S., Kodama, K.P., Jiang, W., Han, Y., Zhang, H., Xu, H. & Zhou, D., 2010. New paleomagnetic results from the Lhasa block: revised estimation of latitudinal shortening across Tibet and implications for dating the India-Asia collision, *Earth planet. Sci. Lett.*, **293**, 396–404, doi:10.1016/j.epsl.2010.03.013.
- Tauxe, L., 2005. Inclination flattening and the geocentric axial dipole hypothesis, *Earth planet. Sci. Lett.*, **233**, 247–261.
- Tauxe, L. & Kent, D.V., 2004. A simplified statistical model for the geomagnetic field and the detection of shallow bias in paleomagnetic inclinations: was the ancient magnetic field dipolar? in *Timescales of the Paleomagnetic Field*, *Geophysical Monograph*, Vol. 145, pp. 101–115, eds Chan-nell, J.E.T., Kent, D.V., Lowrie, W. & Meert, J.G., American Geophysical Union.
- Torsvik, T.H., Dietmar Müller, R., Van Der Voo, R., Steinberger, B. & Gaina, C., 2008. Global plate motion frames: toward a unified model, *Rev. Geophys.*, **46**, RG3004, doi:10.1029/2007RG000227.
- Van Der Voo, R., Spakman, W. & Bijwaard, H., 1999. Tethyan subducted slabs under India, *Earth planet. Sci. Lett.*, **171**, 7–20.
- van Hinsbergen, D.J.J., Hafkenscheid, E., Spakman, W., Meulenkamp, J.E. & Wortel, M.J.R., 2005. Nappe stacking resulting from subduction of oceanic and continental lithosphere below Greece, *Geology*, **33**, 325–328.
- Vandamme, D., 1994. A new method to determine paleosecular variation, *Phys. Earth planet. Inter.*, **85**, 131–142.
- Westphal, M. & Pozzi, J.-P., 1983. Paleomagnetic and plate tectonic constraints on the movement of Tibet, *Tectonophysics*, **98**, 1–10.
- Yin, A. & Harrison, M.T., 2000. Geologic evolution of the Himalayan-Tibetan orogen, *Ann. Rev. Earth planet. Sci.*, **28**, 211–280.
- Yin, A., Dang, Y.-Q., Wang, L.-C., Jiang, W.-M., Zhou, S.-P., Chen, X.-H., Gehrels, G.E. & McRivette, M.W., 2008. Cenozoic tectonic evolution of Qaidam basin and its surrounding regions (Part 1): the southern Qilian Shan-Nan Shan thrust belt and northern Qaidam basin, *Geol. Soc. Am. Bull.*, **120**, 813–846, doi:10.1130/B26180.1.
- Zhu, B., Kidd, W.S.Á.F., Rowley, D.B., Currie, B.S. & Shafique, N., 2005. Age of initiation of the India-Asia collision in the East-Central Himalaya, *J. Geol.*, **113**, 265–285, doi:10.1086/428805.

## SUPPORTING INFORMATION

Additional Supporting Information may be found in the online version of this article:

**Table S1.** Bedding orientations (see Fig. 2).

**Table S2.** Sample Characteristic Remanent Magnetization (ChRM) directions.

**Table S3.** Palaeomagnetic site-mean directions from the Linzizong volcanic flows (see Fig. 4).

**Table S4.** Same as Table S3 for Cretaceous volcanic flows of the Lhasa terrane.

Please note: Wiley-Blackwell are not responsible for the content or functionality of any supporting materials supplied by the authors. Any queries (other than missing material) should be directed to the corresponding author for the article.